

Cite this: DOI: 10.1039/c3gc40683k

Microwave-assisted synthesis of sulfonic acid-functionalized microporous materials for the catalytic etherification of glycerol with isobutene

María Dolores González,^a Pilar Salagre,^a Elena Taboada,^b Jordi Llorca^b and Yolanda Cesteros*^a

Commercial Beta, ZSM-5 and mordenite zeolites and commercial montmorillonite K-10 were successfully sulfonated by a one-step simple method using microwaves. Different amounts of the sulfonating agent were required to maximize the incorporation of sulfonic groups for each structure. This has been related to the different dealumination degree suffered by the starting samples during sulfonation together with the different accessibility of the silanols to the sulfonic groups depending on the arrangement and size of their pores. All optimised sulfonated catalysts showed total conversion and very high selectivity (79–91%) to h-GTBE (glycerol di- and tri-ethers), in spite of their microporosity, due to the incorporation of the sulfonic groups that led to a higher number and strength of Brønsted acid sites. Pore size and arrangement together with the external surface area of the catalysts affected the accessibility of the acid sites to the reactants, explaining the evolution of the catalytic results with time for each structure.

Received 11th April 2013,
Accepted 11th June 2013

DOI: 10.1039/c3gc40683k

www.rsc.org/greenchem

Introduction

Over the last fifteen years, biodiesel is emerging as a competitive alternative to the traditional fossil fuel based diesel. During biodiesel manufacture, by transesterification of vegetable oils with methanol, glycerine (glycerol or 1,2,3-propanetriol) is formed as a by-product in significant amounts (10 weight% of the total product).^{1–3} The price of glycerol is falling as fast as biodiesel plants are being built. Although glycerine has over 1500 known end uses, including applications in cosmetics, pharmaceuticals and food products,^{1,2} it is necessary to find new outlets to convert the surplus of glycerol into high-value-added products that improve the economy of the whole process.^{1,4–8}

One interesting option is the catalytic etherification of glycerol with *tert*-butanol or isobutene to obtain di- and tri-tertiary butyl ethers of glycerol, the so-called “higher ethers” (h-GTBE), which constitute excellent additives with a large potential for diesel and biodiesel reformulation.^{9–11} When h-GTBE was incorporated into standard 30–40% aromatic-containing diesel fuel, emissions of particulate matter,

hydrocarbons, carbon monoxide, and unregulated aldehydes reduced significantly.^{10,11} Etherification of glycerol with isobutene or with *tert*-butanol has been studied in the presence of acid catalysts.^{12–27} Etherification with isobutene yielded higher conversion and selectivity to h-GTBE than etherification with *tert*-butanol.^{14,16}

In the first studies performed with zeolites as catalysts for this reaction, Klepáčová *et al.* reported that the formation of the triether was sterically hindered in H-Beta and H-Y zeolites due to their microporosity.¹⁵ However, in a previous study, we observed the formation of the tri-tertiary butyl ether of glycerol (TTBG) in low amounts when using a fluorinated beta zeolite for the etherification of glycerol with *tert*-butanol.²⁶ Interestingly, the post-synthesis sulfonation of one commercial beta zeolite in one step with microwaves resulted in a catalyst that yielded total conversion and 83% selectivity to h-GTBE, with 15% selectivity to TTBG, after 4 h of reaction for the etherification of glycerol with isobutene.²⁷ Selectivity to h-GTBE and to TTBG increased at higher reaction time (24 h) with this catalyst (91% and 36%, respectively). These catalytic results were better than those obtained with the corresponding sample sulfonated by conventional heating.²⁷ The effect of microwaves on sulfonic acid-functionalization, and therefore on the catalytic activity results, when compared with conventional heating, was mainly related to the homogeneous heating achieved with microwaves. This favoured dealumination of zeolite beta in the acidic medium used during sulfonation and, therefore, the formation of new silanol groups and slightly higher

^aDepartament de Química Física i Inorgànica, Universitat Rovira i Virgili, C/Marcel·lí Domingo s/n, 43007 Tarragona, Spain. E-mail: yolanda.cesteros@urv.cat;

Fax: +34-977559563; Tel: +34-977559571

^bInstitute of Energy Technologies and Centre for Research in Nanoengineering, Universitat Politècnica de Catalunya Diagonal 647, ed. ETSEIB, 08028 Barcelona, Spain

mesoporosity,^{27,29} enhancing the incorporation of the sulfonic acid groups.²⁷ Additionally, the selectivity values were much higher than those obtained by using a macroporous acid-ion exchange resin (Amberlyst-15) as a catalyst for this reaction under the same reaction conditions. From these results, we concluded that the acidity strength significantly influenced the formation of di- and especially tri-ethers of glycerol, independent of the porosity of the catalysts.

Apart from the study commented on above,²⁷ there are no references about the post-synthesis sulfonation of zeolites in one step or about the use of microwaves for the sulfonation of zeolites or other microporous materials (such as smectites) although microwave irradiation has been extensively applied to the synthesis, dealumination, and cation-exchange of zeolites.^{28–30} The use of microwaves considerably decreases the preparation times, with the subsequent energy saving, following one of the principles of green chemistry, and also modifies the samples' properties, which can be of interest for catalysis.

The aim of this work was (a) to explore the effect of using different amounts of the sulfonating agent during the microwave-assisted sulfonic acid-functionalization of three pentasyl-type zeolites (mordenite, ZSM-5 and Beta) on the catalytic etherification of glycerol with isobutene; (b) to find the optimum extent of sulfonation for each zeolite to maximize the obtention of the product of interest (h-GTBE); and (c) to correlate the possible zeolite dealumination that occurred during sulfonic acid-functionalization with the extent of sulfonation, and the pore size and arrangement, and the external surface area of the three zeolite structures with the obtention of the bulkier triether. One commercial montmorillonite K-10 was also sulfonated with microwaves and tested for this reaction for comparison. There are no references about sulfonation of smectites with microwaves.

Experimental

Catalyst preparation

Three commercial pentasyl-type zeolites were sulfonic acid-functionalized in one step by using microwaves (Milestone ETHOS-TOUCH CONTROL equipped with a temperature controller). Na-Mordenite (Zeolyst, Si/Al = 6.5, CBV 10A Lot No. 1822-50), Na-Beta (Zeochem, Si/Al = 10, PB Lot No. 6000186) and Na-ZSM-5 (Zeochem, Si/Al = 20, PZ-2/40 Lot No. 6002827,01) were designated as M, B and Z, respectively.

2 g of commercial zeolite were treated with different amounts of a 2-(4-chlorosulfonylphenyl)ethyltrimethoxysilane (CSPTMS) solution in methylene chloride (50 wt%, Gelest) in a 2 M HCl solution by refluxing with microwaves at 40 °C for 2 h. Sulfonic acid-functionalized zeolites were called S-B(x), S-Z(x), S-M(x), where x is the amount (in grams) of the CSPTMS used. For example, the sample S-M(1.4) was obtained by treating commercial mordenite with 1.4 g of CSPTMS. Samples were filtered, washed with deionised water and dried overnight.

Additionally, 2 g of commercial montmorillonite K-10 (Sigma-Aldrich, Si/Al = 2.7), here named as Mont, were treated

with 1.4 g of CSPTMS in a 2 M HCl solution by refluxing with microwaves at 40 °C for 2 h (the sample S-Mont(1.4)). Samples were filtered, washed with deionised water and dried overnight.

Catalyst characterization

X-ray diffraction (XRD) patterns of the samples were obtained with a Siemens D5000 diffractometer using nickel-filtered Cu K α radiation. Samples were dusted on double-sided sticky tape and mounted on glass microscope slides. The patterns were recorded over a range of 2θ angles from 5° to 40° and crystalline phases were identified using the Joint Committee on Powder Diffraction Standards (JCPDS) files (43-0171, 48-0074, 37-359 correspond to mordenite, beta and ZSM-5, respectively). Crystallinity of the modified mordenites was determined by comparing the sum of the peak areas of (150), (202), (350) and (402) ($22\text{--}32^\circ 2\theta$) with respect to commercial Na-mordenite. Crystallinity of the modified ZSM-5 samples was calculated using the (051) peak intensity compared with the parent zeolite sample. The integrated intensity of the signal at $2\theta = 22.4^\circ$ was used to evaluate the crystallinity of beta samples.

Textural characterization of the solids was performed by N₂ ($\sigma_{N_2} = 0.162 \text{ nm}^2$) adsorption–desorption at 77 K using a Quadrasorb SI surface analyser. Before measurements all samples were outgassed at 573 K for 6 h. The BET specific surface areas were calculated using adsorption data in the relative pressure range $0 < P/P_0 < 0.1$. Micropore and external surface areas were obtained by *t*-plot analysis of the adsorption data in the $3.5 \leq t \leq 5 \text{ \AA}$ *t* range by adopting the de Boer reference isotherm equation, whereas pore volumes and pore size distributions were determined by the Barrett–Joyner–Halenda (BJH) method.

XP spectra (XPS) were collected at a pressure below $5 \times 10^{-7} \text{ Pa}$ with a SPECS system using an Al anode XR50 X-ray source (150 W) and a 9-channel Phoibos 150 MCD detector with a pass energy of 25 eV at 0.1 eV steps. Quantification of surface elements was carried out using Shirley baselines and Gaussian–Lorentzian (1 : 1) lineshapes. Binding energy values were referred to the C1s adventitious signal.

Elemental analyses of the samples were obtained with a Philips PW-2400 sequential XRF analyzer with Philips Super Q software. All measurements were made in triplicate.

Scanning electron microscopy (SEM) was performed on a scanning electron microscope, JEOL JSM6400, operating at an accelerating voltage of 25 kV and a work distance of 10 mm, and a magnification of 2000–50 000.

Thermogravimetric analyses (TGA) were performed with a TA Instruments equipment from 50 °C to 800 °C at 10 °C min⁻¹ under airflow.

Infrared spectra were recorded on a Bruker-Equinox-55 FTIR spectrometer with a MCT detector using a DRIFT cell connected to a temperature controller. Samples were dehydrated at 623 K for 2 h under nitrogen. The spectra were then acquired at this temperature by accumulating 64 scans at 4 cm⁻¹ resolution in the range of 400–4000 cm⁻¹.

Acid capacity was measured by the determination of cation-exchange capacities using aqueous sodium chloride (2 M) solutions as cationic-exchange agents. The released protons were then potentiometrically titrated.³¹

Catalytic activity

Etherification experiments were performed in the liquid phase in a stainless steel stirred autoclave (150 mL) equipped with a temperature controller and a pressure gauge. Stirring was fixed for all experiments at 1200 rpm to avoid external diffusion limitations. Liquid phase pressurized isobutene (glycerol–isobutene molar ratio of 0.25) was injected into the reactor, previously charged with glycerol and a catalyst (0.5 g), using nitrogen at 10 bar as a pushing agent. The temperature was then raised to 75 °C and the pressure increased accordingly following the liquid–vapour equilibrium. Catalytic experiments were made at 4, 24 and 48 h. The reaction products were analyzed by gas chromatography using a chromatograph model Shimadzu GC-2010 equipped with a SupraWax-280 column and a FID detector.

Glycerol conversion and selectivity to MTBG (glycerol monoethers) were determined from calibration lines obtained from commercial products. For DTBG (glycerol diethers) and TTBG (glycerol triether), which were not available commercially, we isolated them from the products of the etherification reaction using column chromatography (1:9 ethyl acetate–hexane) and identified them by ¹³C and ¹H NMR for proper quantification.^{27,32}

Results and discussion

Catalyst characterization

XRD patterns of sulfonated zeolites revealed that, after sulfonation, the three zeolites maintained their structure (*e.g.*

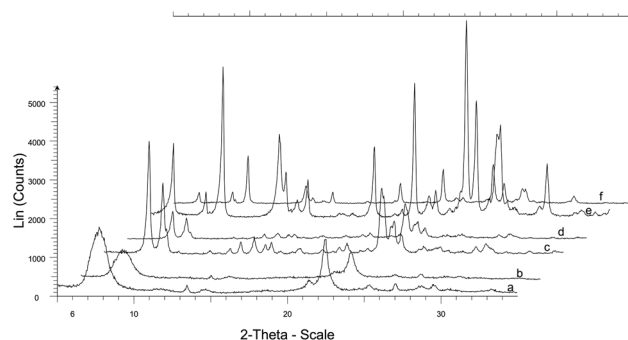


Fig. 1 XRD patterns of (a) B, (b) S-B(1.4), (c) Z, (d) S-Z(1.8), (e) M and (f) S-M (1.6) samples.

Fig. 1) although some decrease of crystallinity was observed for all of them (Table 1).

N₂ adsorption–desorption isotherms were type I for all the zeolite samples, before and after sulfonation (*e.g.* Fig. 2), attributed to microporous materials, according to the Brunauer, Deming, Deming and Teller classification.³³ All sulfonated beta samples showed lower surface areas, and on the whole, lower pore volumes than commercial beta (Table 1). In contrast, sulfonated mordenites exhibited higher surface areas and higher pore volumes than commercial mordenite (Table 1) whereas sulfonated ZSM-5 zeolites had slightly higher surface areas than commercial ZSM-5 except for the ZSM-5 sulfonated with higher amounts of sulfonic agent where a considerable decrease of surface area and pore volume was observed (Table 1, Fig. 2). There are several factors that can contribute to explain these results: the partial dealumination suffered by the zeolites (the extent of which depends on the zeolite structure) because of the acidic medium used during sulfonation, the loss of crystallinity observed for the sulfonated samples, and the partial blockage of the pores by the sulfonic groups.

Table 1 Characterization of catalysts

Catalysts	Crystallinity ^a (%)	BET area (m ² g ⁻¹)	External surface area (m ² g ⁻¹)	Pore volume (cc g ⁻¹)	Sulfur content ^b	Acid capacity ^c (meq H ⁺ g ⁻¹)
B	100	573	203	0.23	—	—
S-B(0.7)	50	502	152	0.20	0.31	0.30
S-B(1.0)	49	501	165	0.21	0.40	0.42
S-B(1.4)	45	505	183	0.24	0.70	0.72
S-B(1.8)	37	249	87	0.16	0.74	0.74
S-B(2.2)	30	88	36	0.04	0.77	0.76
Z	100	300	87	0.06	—	—
S-Z(0.7)	50	355	112	0.07	0.14	0.17
S-Z(1.4)	54	345	111	0.05	0.16	0.26
S-Z(1.8)	53	213	79	0.02	0.68	0.52
S-Z(2.2)	44	92	48	0.01	0.70	0.54
M	100	413	42	0.10	—	—
S-M(1.4)	31	529	67	0.15	0.14	0.62
S-M(1.6)	29	426	58	0.07	0.60	0.82
S-M(1.8)	32	500	60	0.12	0.72	0.77
S-M(2.2)	30	489	55	0.11	0.70	0.62
Mont	—	233	233	0.36	—	—
S-Mont(1.4)	—	125	125	0.19	0.71	0.77

^a Calculated from XRD patterns. ^b (mmol organic sulfonic acid group per g sample) calculated from TGA. ^c Obtained by potentiometric titration.

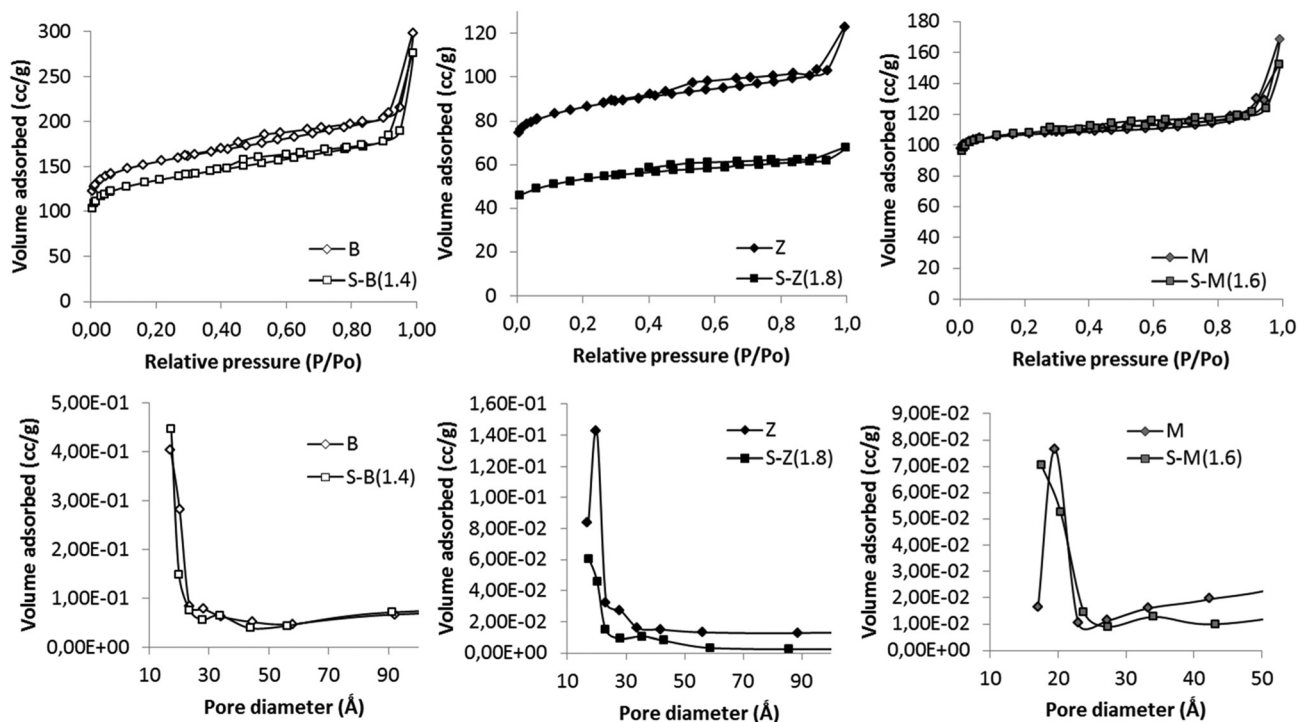


Fig. 2 Nitrogen adsorption-desorption isotherms and pore size distribution of B, S-B(1.4), Z, S-Z(1.8), M and S-M(1.6).

Zeolite beta has a three-dimensional 12-ring pore system (straight channels of diameter 6.6×6.7 Å and sinusoidal channels of diameter 5.6×5.6 Å) and, because of this property, the framework is very flexible. Zeolite mordenite has a one-dimensional pore system with the main 12-ring channels of diameter 6.7×7.0 Å and compressed 8-ring channels of diameter 2.6×5.7 Å, whereas ZSM-5 has a three-dimensional 10-ring pore system with channels of diameter 5.1×5.5 Å. Both these structures are less flexible than beta, and consequently, it is more difficult to dealuminate them. Additionally, zeolite beta crystallizes with many stacking faults³⁴ while mordenite samples, although less frequently, may also have structurally related stacking faults.³⁵ Stacking faults increase the probability of the presence of defect sites in the framework. Thus, beta zeolite is easier to dealuminate than mordenite and mordenite is easier to dealuminate than ZSM-5, which always shows very low dealumination.^{29,36} In a previous study, we also concluded that the use of microwaves led to faster dealumination than conventional heating for the three zeolites.²⁹

Therefore, the higher surface areas observed for the sulfonated mordenite samples could be mainly associated with the loss of aluminium in the zeolite structure, due to the acidic medium used during sulfonation, which results in higher mesoporosity and higher surface area, as reported before for partially dealuminated mordenites.^{29,37,38} On the other hand, for sulfonated beta samples, although dealumination was higher than for the sulfonated mordenites, the surface area and pore volume decreased after sulfonation for all samples. It is well known that the loss of crystallinity that occurred during dealumination of beta, which has many stacking faults, results

in a decrease of its surface area.³⁹ The lowest surface area obtained for S-B(2.2) can be additionally related to the partial blockage of the pores by the sulfonic acid groups. Finally, the low dealumination of ZSM-5 practically did not affect the surface areas and pore volumes of the sulfonated samples, and only when the amount of the sulfonating agent was higher, lower surface areas and lower pore volumes were observed.

Scanning electron microscopy was used to monitor the morphologies and sizes of the particles of the sulfonic acid-functionalized samples with respect to their corresponding starting commercial zeolites (Fig. 3). Sulfonated mordenite and beta samples appeared less agglomerated, with less densely packed crystallites, than their corresponding

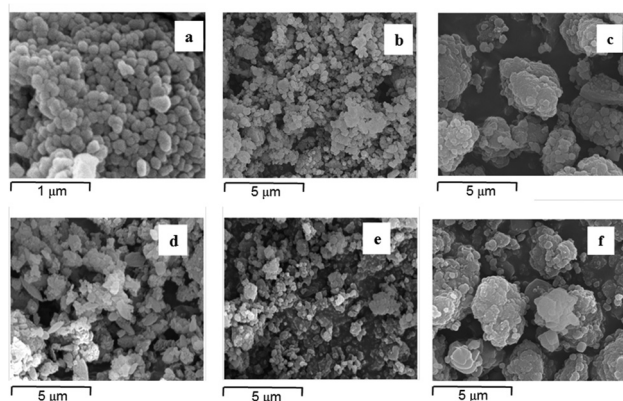


Fig. 3 Scanning electron micrographs of samples (a) M, (b) B, (c) Z, (d) S-M(1.6), (e) S-B(1.4) and (f) S-Z(1.8).

commercial ones, whereas the micrographs of ZSM-5 samples were very similar.

The thermogravimetric analysis (TGA) technique was used to confirm and quantify the introduction of the sulfonic acid groups since the weight loss observed between 360 °C and 660 °C in the TGA for all the organosulfonated samples has been related in the literature to the loss of organosulfonic acid groups,³¹ allowing us to calculate the mmol organic sulfonic acid group per g sample (Table 1). This is the first time that post-synthesis sulfonation of commercial ZSM-5 and mordenite in one-step has been reported. Additionally, this is also the first time that microwaves have been used for sulfonating these two zeolites.

X-ray photoelectron spectroscopy (XPS) is useful in evaluating qualitatively the type of sulfur species and in measuring quantitatively the sulfonic acid groups near the surface region.^{40,41} The S 2p XP spectra of the most representative sulfonated samples (Fig. 4) only showed one peak at *ca.* 168–169 eV associated with sulfate (S⁶⁺) species due to sulfonic (–SO₃H) acid groups.^{40,41} Therefore, XPS confirmed sulfonation of zeolites in agreement with TGA results. The S/Si surface atomic ratio, calculated from XPS, was similar for the three sulfonated zeolites (Table 2). The Si/Al surface atomic ratios, obtained from XPS, sample and agree with the sulfur contents obtained by TGA and also confirmed that beta suffered higher dealumination than mordenite and ZSM-5 during sulfonation.

Finally, the acidity of the sulfonated zeolites, determined potentiometrically, agrees with the TGA results, since, on the whole, the sulfonated samples which had higher amounts of sulfonic acid groups led to higher acidity, as expected (Table 1).

Taking into account that the main difficulty of introducing bulky organic species into zeolites is their microporous structure together with the lack of reactant silanol groups (≡Si–OH),⁴² an important key to understand these good zeolite sulfonation results is that the zeolite dealumination occurred under the acidic conditions used during sulfonation. It is well known that during dealumination, the loss of aluminum of the zeolite framework led to the formation of silanol groups.⁴³ We believe that these new silanol groups can react with the

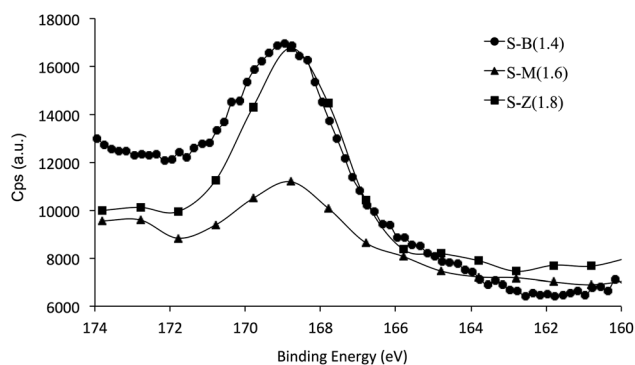


Fig. 4 XP spectra of samples S-B(1.4), S-Z(1.8) and S-M(1.6) in the S2p core level region.

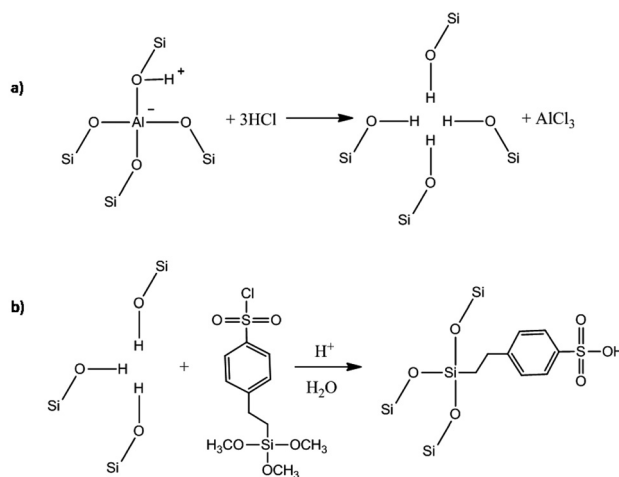
Table 2 Elemental analysis of several representative catalysts

Catalysts	S/Si atomic ratio ^a	Si/Al atomic ratio ^a	Si/Al bulk ratio ^b
B	—	—	10
S-B(1.4)	0.06	69	71
Z	—	—	20
S-Z(1.8)	0.05	29	28
M	—	—	6.5
S-M(1.6)	0.06	22	26
Mont	—	—	2.7
S-Mont(1.4)	0.06	4.5	5.3

^a Calculated from XP spectra. ^b Determined from XRF.

sulfonating agent to form the sulfonic acid groups (Scheme 1) as previously observed for sulfonated beta zeolite.³¹ Fig. 5 shows the FTIR spectra of commercial mordenite, a partially dealuminated mordenite sample (DAM), which was obtained by treatment of commercial mordenite in HCl 2 M for 15 min, and the sulfonated mordenite sample S-M(1.6). As we can observe, there was an increase in the intensity of the silanol band (around 3745 cm⁻¹) for the partially dealuminated sample (DAM) whereas after sulfonation, the silanol band decreased as a consequence of the reaction of the silanol groups, formed during dealumination, with the organo-sulfonating agent.

The optimum amount of the sulfonating agent was different for each zeolite structure. Zeolite beta, which is easier to dealuminate,^{29,36} can generate more silanol groups. Additionally, the arrangement and size of the pores in this zeolite allow higher accessibility of the silanol groups to the sulfonating agent. Therefore, the higher amount of silanols together with their higher accessibility explains the lower amount of CSPTMS required to achieve the optimum extent of sulfonation for this zeolite. Thus, for beta zeolite, the optimum amount was 1.4 g, since at higher CSPTMS amounts, the sulfur content slightly increased but BET areas and external surface areas dramatically decreased (Table 1). In the same



Scheme 1 (a) Formation of silanols during dealumination in acidic medium and (b) reaction of silanols with CSPTMS to form the sulfonating groups.

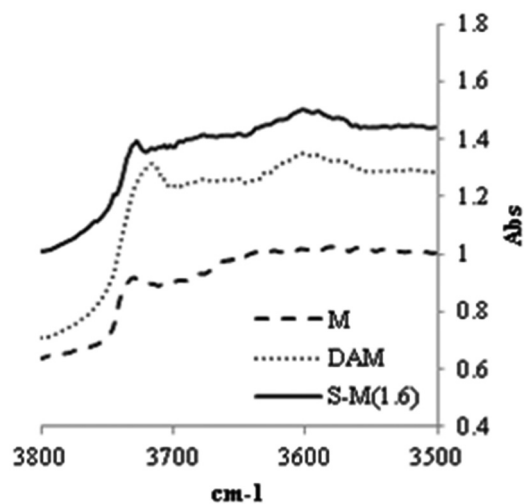


Fig. 5 FTIR spectra of commercial mordenite, partially dealuminated mordenite, and the sulfonated sample S-M(1.6).

way, mordenite is easier to dealuminate than ZSM-5,^{29,36} as commented above. This involves a higher formation of silanol groups in mordenite than in ZSM-5, and therefore, fewer amounts of CSPTMS (1.6) were necessary to obtain the optimum extent of sulfonation. At higher CSPTMS amounts, the sulfur content slightly increased but the accessibility of the sulfonic acid groups was lower, as deduced from the lower acidity values found (Table 1). Finally, the very low dealumination of ZSM-5 can justify the higher CSPTMS content added to obtain the optimised sulfonated sample (1.8). At higher CSPTMS amounts, the sulfur content slightly increased but the BET and external surface areas decreased (Table 1). These optimum amounts of the sulfonating agent for each zeolite will be confirmed and correlated later with the catalytic results.

Montmorillonite is a clay of the smectite group with the general formula $[\text{Si}_8(\text{Al}_{4-x}\text{Mg}_x)(\text{OH})_4\text{O}_{20}]\text{M}^{n+}_{x/n}\cdot m\text{H}_2\text{O}$. These layered materials are microporous, like zeolites. Sulfonated montmorillonite K-10 maintained the starting smectite structure, as observed by XRD (Fig. 6), with some decrease of crystallinity (Table 1). After sulfonation, we observed a decrease of the surface area and the pore volume (Table 1). This can be

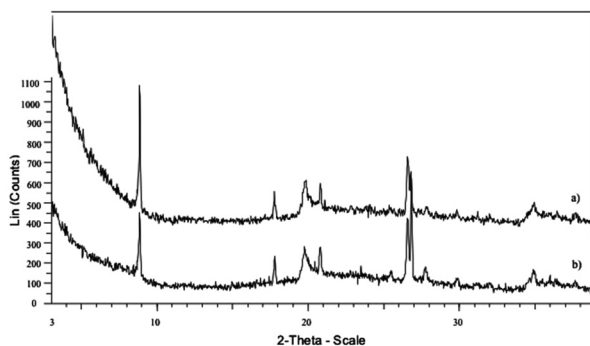


Fig. 6 XRD pattern of samples (a) Mont and (b) S-Mont(1.4).

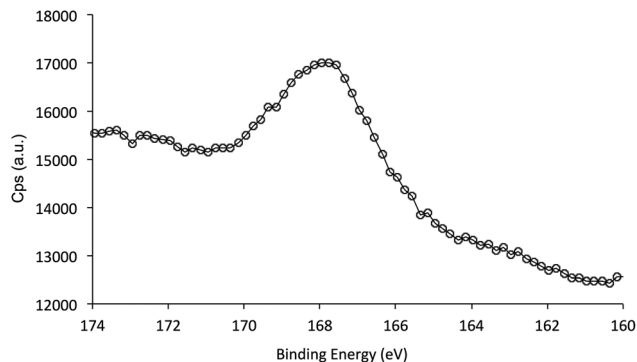


Fig. 7 XP spectra of the sample S-Mont(1.4) in the S2p core level region.

explained because of the introduction of sulfonic acid groups according to the sulfur content related to sulfonic acid groups, determined by TGA (Table 1), the S/Si surface atomic ratio obtained from the XP spectrum (Table 2, Fig. 7) and its higher acidity (Table 1) potentiometrically evaluated. This sample also exhibited slight dealumination after sulfonation (Table 2).

Catalytic activity

Tables 3–5 show the catalytic activity results of beta, ZSM-5 and mordenite catalysts, respectively, for the etherification reaction of glycerol with isobutene. The reaction products obtained were mono-*tert*-butyl glycerol ether (MTBG), di-*tert*-butyl glycerol ether (DTBG) and tri-*tert*-butyl glycerol ether (TTBG). Besides, diisobutylene was detected in low amounts for most of the sulfonated samples. All sulfonated catalysts maintained the sulfur content after reaction, as determined by TGA. This confirms that there was no leaching of the sulfonic acid groups during reaction.

Zeolite Na-beta was more active and selective to h-GTBE than Na-ZSM-5 and Na-mordenite, as deduced by comparing the activity values after 24 h of reaction (Tables 3–5). This behaviour was previously observed specifically when the same commercial Na-zeolites used in this study were tested for the glycerol etherification with *tert*-butanol.²⁶ One important feature to remark is that triether was not detected for Na-mordenite or Na-ZSM-5 and in very low amounts (1%) for Na-Beta (Table 3). This has been attributed to steric hindrance effects because of the microporosity of the zeolites¹⁵ but based on our previous results we believe that the formation of the glycerol triether could be mainly related to the presence of stronger Brønsted acid sites,^{26,27} as confirmed regarding the catalytic results of the sulfonated zeolites presented here.

All sulfonated zeolite catalysts showed higher conversion than their corresponding non-sulfonated zeolites due to the presence of the sulfonic acid groups. Sulfonated beta catalysts exhibited a very high conversion (almost total) after only 4 h of reaction (Table 3). Selectivity to h-GTBE values increased when the acidity due to the sulfonic acid groups increased (Table 1). Thus, the best catalytic results were obtained with the catalyst with the optimum amount of sulfonic groups, SB(1.4), which showed total conversion and 83% selectivity to h-GTBE with

Table 3 Catalytic activity of Beta catalysts for the etherification of glycerol with isobutene after 4 h

Catalyst	Conversion (%)	Selectivity to MTBG ^a (%)	Selectivity to h-GTBE ^b (%)	DIB ^c (%)
B	44	32	68 (1)	5.3
S-B(0.7)	97	73	26 (1)	3.0
S-B(1)	93	60	40 (1)	1.9
S-B(1.4)	100	17	83 (15)	2.0
S-B(2.2)	98	33	67 (7)	1.0
B ^e	49	39	61 (2)	6.1
S-B(1.4) ^d	100	9	91 (36)	9.4
S-B(2.2) ^d	99	23	77 (18)	2.5
S-B(1.4) ^e	100	10	90 (35)	9.3

^a MTBG: glycerol monoethers. ^b h-GTBE: glycerol diethers + glycerol triether. In parentheses, selectivity to glycerol triether (%). ^c DIB: diisobutylene. ^d Reaction time: 24 h. ^e Reaction time: 48 h.

Table 4 Catalytic activity of ZSM-5 catalysts for the etherification of glycerol with isobutene after 24 h

Catalyst	Conversion (%)	Selectivity to MTBG ^a (%)	Selectivity to h-GTBE ^b (%)	DIB ^c (%)
Z	25	83	17 (0)	0
S-Z(0.7)	50	86	14 (2)	5.5
S-Z(1.4)	54	92	9 (0)	0.1
S-Z(1.8)	100	16	84 (28)	3.9
S-Z(2.2)	95	36	64 (6)	2.2
S-Z(0.7) ^d	37	90	10 (0)	0.9
S-Z(1.8) ^d	99	28	72 (9)	1.2
S-Z(1.8) ^e	98	17	83 (24)	4.5

^a MTBG: glycerol monoethers. ^b h-GTBE: glycerol diethers + glycerol triether. In parentheses, selectivity to glycerol triether (%). ^c DIB: diisobutylene. ^d Reaction time: 4 h. ^e Reaction time: 48 h.

Table 5 Catalytic activity of mordenite catalysts for the etherification of glycerol with isobutene after 48 h

Catalyst	Conversion (%)	Selectivity to MTBG ^a (%)	Selectivity to h-GTBE ^b (%)	DIB ^c (%)
M	37	84	16 (0)	0
S-M(1.4)	95	51	49 (8)	3.3
S-M(1.6)	99	21	79 (21)	1.6
S-M(1.8)	94	61	39 (7)	3.4
S-M(2.2)	98	50	50 (5)	3.7
S-M(1.6) ^d	71	73	27 (0)	0.7
S-M(1.8) ^d	34	95	5 (0)	0
M ^e	15	92	8 (0)	0

^a MTBG: glycerol monoethers. ^b h-GTBE: glycerol diethers + glycerol triether. In parentheses, selectivity to glycerol triether (%). ^c DIB: diisobutylene. ^d Reaction time: 4 h. ^e Reaction time: 24 h.

15% selectivity to the triether (Table 3). When this catalyst was tested at a longer reaction time (24 h), the selectivity to h-GTBE improved until 91% with 36% selectivity to the triether maintaining total conversion. This means that when glycerol conversion stopped the isobutene molecules remaining in the reaction medium react with monoethers and diethers formed previously evolving with time to higher selectivity to the di- and triether. However, after 48 h of reaction, the selectivity

values practically did not change. At higher sulfur content (S-B(2.2)), the selectivity to h-GTBE decreased because of the lower acidity and lower BET and external surface area of this catalyst (Table 1) due to the excess of the sulfonating agent that is blocking the pores, hindering the formation of the bulkier products, di- and triethers. At higher reaction time (24 h), the selectivity to h-GTBE and to the triether of S-B(2.2) catalyst increased, following the same tendency as that observed for S-B(1.4).

Regarding the catalytic activity of sulfonated ZSM-5 catalysts, the best catalytic results were obtained after 24 h of reaction with the catalyst S-Z(1.8), with the optimum incorporation of sulfonic groups, resulting in total conversion, selectivity to h-GTBE of 84% and selectivity to the triether of 28% (Table 4). These results can be explained by the higher acidity of this catalyst because of the presence of higher amounts of sulfonic acid groups (Table 1). At shorter or longer reaction times, the catalytic results did not improve.

Finally, sulfonated mordenite catalysts required 48 h of reaction to achieve almost total conversion and the highest selectivity to h-GTBE and to the triether values (79% and 21%, respectively) (Table 5). At lower reaction times, conversion and selectivity to h-GTBE were lower and TTBG was not detected. The catalytic differences observed between catalysts S-M(1.6) and S-M(1.8) can be mainly attributed to the higher amount of acid sites of S-M(1.6), and probably the higher accessibility of its sulfonic acid groups regarding its lower sulphur content (Table 1). These catalytic results can be attributed to the different pore size distribution and the lower external surface area of mordenite catalysts compared with beta or ZSM-5 catalysts (Table 1).

Interestingly, although the catalyst S-M(1.8) had slightly higher sulfur content, and therefore slightly higher acidity than catalyst S-B(1.4), the selectivity to h-GTBE was lower at the same reaction conditions (Tables 3 and 5). This confirms that, in addition to the acidity, other factors, such as the pore size distribution of the zeolite structure (beta is a very flexible structure and has a 12-ring three-dimensional pore system whereas mordenite has a one-dimensional pore system) and, especially, the external surface area (183 m² g⁻¹ of S-B(1.4) versus 60 m² g⁻¹ of S-M(1.8), Table 1) constituted important key factors, which determined the catalytic activity. This also explains the lower reaction times needed by Beta catalysts to achieve good catalytic results.

All sulfonated catalysts maintained the sulfur content after reaction, as determined by TGA. This confirms that there was no leaching of the sulfonic acid groups during reaction. However, from N₂ adsorption-desorption results, we observed a decrease of the surface area after reaction for all of them, especially after a longer reaction time. This can be explained by the presence of reagents and reaction products in the pores. This decreases the accessibility of the reagents to the acid sites.

Catalytic life of the best catalysts (S-B(1.4), S-Z(1.8) and S-M(1.6)) was evaluated from three consecutive runs performed reusing catalysts under the same reaction conditions as those

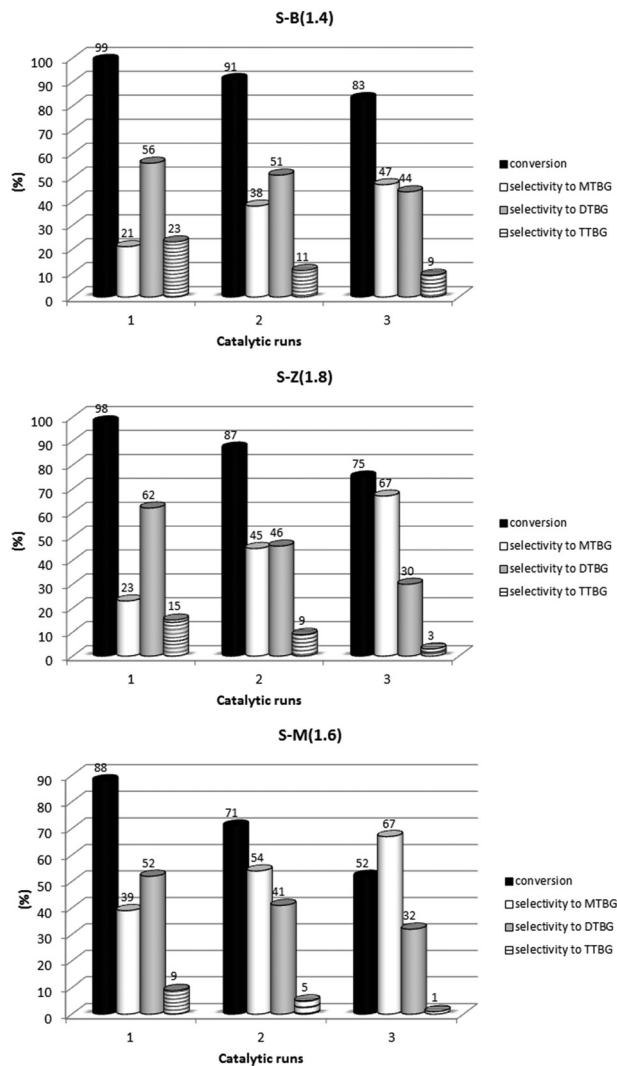


Fig. 8 Catalytic lifetime of the best catalysts. MTBG: glycerol monoethers; DTBG: glycerol diethers; TTBG: glycerol triether. Reaction time for each run: 24 h except for S-M(1.6) which was 48 h.

used in their best catalytic test (Fig. 8). After each catalytic run, recovering of the catalyst was performed by filtration, washing in ethanol and acetone at room temperature and dried before reaction. After the three consecutive catalytic runs, the general trend of the catalysts is a progressive decrease of conversion and selectivity to h-GTBE values, in the following order: S-B (1.4) < S-Z(1.8) < S-M(1.6). This can be related to the structure characteristics of each zeolite since beta zeolite and ZSM-5 have a three-dimensional pore system whereas mordenite has a one-dimensional one. After each catalytic run, we observed a smaller decrease of surface area for sulfonated beta compared with sulfonated ZSM-5 or sulfonated mordenite. Also, sulfonated beta recovered to a higher extent the surface area after washing/drying than the other two catalysts, although after each catalytic run the recovery of surface area was progressively lower, explaining the catalytic activity variations observed in Fig. 8.

Table 6 Catalytic activity of montmorillonite catalysts for the etherification of glycerol with isobutene after 24 h

Catalyst	Conversion (%)	Selectivity to MTBG ^a (%)	Selectivity to h-GTBE ^b (%)	DIB ^c (%)
Mont	90	69	30 (1)	0.3
S-Mont(1.4)	100	16	84 (28)	4.5
S-Mont(1.4) ^d	99	16	84 (14)	15.0

^a MTBG: glycerol monoethers. ^b h-GTBE: glycerol diethers + glycerol triether. In parentheses, selectivity to glycerol triether (%). ^c DIB: diisobutylene. ^d Reaction time: 4 h.

Commercial montmorillonite K-10 showed high conversion but low selectivity to h-GTBE. However, after sulfonation, in addition to the increase of conversion, a high selectivity to h-GTBE was obtained from 4 h of reaction, doubling the selectivity to TTBG after 24 h of reaction (Table 6).

From all these results, we can confirm that it is possible to obtain high selectivity values to h-GTBE, including the formation of the bulkier triether, in microporous materials, such as zeolites and smectites by increasing the number and especially the strength of the Brønsted acid sites together with the use of the appropriate reaction times that facilitate the consecutive transformations of glycerol to the monoether, the monoether to diethers, and finally the diethers to the triether. We also concluded that the accessibility of the reactants to the active sites depending on the pore size and arrangement and especially the external surface area of each structure also have a significant influence in the catalytic results, especially in the optimization of the reaction time to obtain the maxima selectivity to h-GTBE. It is important to remark that the best catalytic results obtained for each sulfonated material are better than those obtained with an Amberlyst-15 catalyst, a macroporous acid resin widely used for this reaction, which was tested under the same reaction conditions.²⁷ Amberlyst-15 showed 35% selectivity to h-GTBE (3% TTBG) for a 73% conversion after 4 h of reaction, and 77% selectivity to h-GTBE (19% TTBG) for a 99% conversion after 24 h of reaction.²⁷

Conclusions

Three commercial Beta, ZSM-5 and mordenite zeolites and one commercial montmorillonite K-10 were successfully sulfonated by a one-step simple method using microwaves.

The highest incorporation of sulfonic acid groups was achieved with different amounts of sulfonating agent for each structure. This has been explained by the different dealumination degree suffered by the starting samples under the acidic conditions used during sulfonation since higher dealumination involved the formation of higher amounts of silanol groups that can react with the sulfonating agent to form the sulfonic acid groups. Additionally, we observed that the arrangement and size of the pores also affected the accessibility of the silanol groups to the sulfonating agent.

The presence of the sulfonic acid groups, which resulted in higher number and strength of Brønsted acid sites than those of the starting commercial materials, resulted in high activity and high selectivity to h-GTBE catalysts, in spite of their microporosity, for the etherification of glycerol with isobutene. The optimised catalytic results were obtained by beta sulfonated with 1.4 g of a sulfonating agent with total conversion and 91% selectivity to h-GTBE with 36% of TTBG after 24 h of reaction followed by ZSM-5 sulfonated with 1.8 g of a sulfonating agent and montmorillonite sulfonated with 1.4 g of a sulfonating agent both with total conversion and 84% selectivity to h-GTBE with 28% of TTBG after 24 h of reaction. Finally, mordenite sulfonated with 1.6 g of a sulfonating agent led to 99% conversion and 79% selectivity to h-GTBE with 21% of TTBG after 48 h of reaction. These catalytic results are better than those obtained with an Amberlyst-15 catalyst, a macroporous acid resin widely used for this reaction.

Sulfonated mordenite catalysts required higher reaction time than the other catalysts to achieve the optimal conversion and selectivity to h-GTBE values. This can be related to the one-dimensional pore system of the mordenite, and its lower external surface area, which makes it difficult for the reactants to access the acid sites. Moreover, we observed higher selectivity to h-GTBE with an optimised sulfonated beta catalyst that had less acidity than an optimised sulfonated ZSM-5 catalyst under the same reaction conditions although both zeolites have a tridimensional structure. The higher external surface area of beta catalysts can justify this result. Therefore, the size and arrangement of the pores together with the external surface area also affected the catalytic results.

Acknowledgements

The authors are grateful for the financial support from the Ministerio de Ciencia e Innovación and the FEDER funds (CTQ2008-04433/PPQ and CTQ2011-24610). Dolores González acknowledges the Ministerio de Educación y Ciencia for a FPU grant (AP2007-03789). Jordi Llorca is grateful to the ICREA Academia program.

Notes and references

- M. Pagliaro, R. Ciriminna, H. Kimura, M. Rossi and C. Della Pina, *Angew. Chem., Int. Ed.*, 2007, **46**, 4434.
- R. D'Aquino and G. Ondrey, *Chem. Eng.*, 2007, **114**, 31.
- J. Feng, M. Yuan, H. Chen and X. Li, *Prog. Chem.*, 2007, **19**, 651.
- A. Behr, J. Eilting, K. Irawadi, J. Leschinski and F. Lindner, *Green Chem.*, 2008, **10**, 13.
- J. Barrault and F. Jerome, *Eur. J. Lipid Sci. Technol.*, 2008, **110**, 825.
- M. Pagliaro, R. Ciriminna, H. Kimura, M. Rossi and C. Della Pina, *Eur. J. Lipid Sci. Technol.*, 2009, **111**, 788.
- N. Rahmat, A. Z. Abdullah and A. R. Mohamed, *Renew. Sustain. Energy Rev.*, 2010, **14**, 987.
- M. O. Guerrero-Pérez, J. M. Rosas, J. Bedia, J. Rodríguez-Mirasol and T. Cordero, *Rec. Patents Chem. Eng.*, 2009, **2**, 11.
- T. S. Viinikainen, R. S. Karinen and A. O. Krause, in *Conversion of Glycerol into traffic Fuels. Catalysis for Renewables: From Feedstock to Energy Production*, ed. G. Centi and R. A. van Santen, Wiley-VCH Verlag GmbH and Co. KGaA, Weinheim, 2007.
- F. J. Liotta Jr., L. J. Karas and H. Kesling, *US Pat*, 5308365, 1994, to ARCO Chemical Technology, L.P.
- M. Marchionna, R. Patrini, D. Sanfilippo, A. Paggini, F. Giavazzi and L. Pellegrini, *Stud. Surf. Sci. Catal.*, 2001, **136**, 489.
- R. S. Karinen and A. O. I. Krause, *Appl. Catal., A*, 2006, **306**, 128.
- K. Klepáčová, D. Mravec, E. Hájeková and M. Bajus, *Petrol. Coal*, 2003, **45**, 54.
- K. Klepáčová, D. Mravec and M. Bajus, *Appl. Catal., A*, 2005, **294**, 141.
- K. Klepáčová, D. Mravec, A. Kaszony and M. Bajus, *Appl. Catal., A*, 2007, **328**, 1.
- J. A. Melero, G. Vicente, G. Morales, M. Paniagua, J. M. Moreno, R. Roldán, A. Ezquerro and C. Pérez, *Appl. Catal., A*, 2008, **346**, 44.
- J. A. Melero, J. Iglesias and G. Morales, *Green Chem.*, 2009, **11**, 1285.
- M. Di Serio, L. Casale, R. Tesser and E. Santacesaria, *Energy Fuels*, 2010, **24**, 4668.
- H. J. Lee, D. Seung, K. S. Jung, H. Kim and I. N. Filimonov, *Appl. Catal., A*, 2010, **390**, 235.
- L. Xiao, J. Mao, J. Zhou, X. Guo and S. Zhang, *Appl. Catal., A*, 2011, **393**, 88.
- W. Zhao, B. Yang, C. Yi, Z. Lei and J. Xu, *Ind. Eng. Chem. Res.*, 2010, **49**, 12399.
- P. M. Slomkiewicz, *Appl. Catal., A*, 2006, **313**, 74.
- R. Luque, V. Budarin, J. H. Clark and D. Macquarrie, *Appl. Catal., B*, 2008, **82**, 157.
- F. Frusteri, F. Arena, G. Bonura, C. Cannilla, L. Spadaro and O. Di Blasi, *Appl. Catal., A*, 2009, **367**, 77.
- N. Ozbay, N. Oktar and N. A. Tapan, *Int. J. Chem. React. Eng.*, 2010, **8**, A18, 1.
- M. D. González, Y. Cesteros and P. Salagre, *Appl. Catal., A*, 2013, **450**, 178.
- M. D. González, Y. Cesteros, P. Salagre and J. Llorca, *J. Catal.*, 2012, **290**, 202.
- H. M. Kingston and S. J. Haswell, in *Microwave-Enhanced Chemistry Fundamentals, Sample Preparation and Applications*, American Chemical Society, Washington, DC, 1997.
- M. D. González, Y. Cesteros and P. Salagre, *Microporous Mesoporous Mater.*, 2011, **144**, 162.
- O. Bergadà, E. Boix, P. Salagre, Y. Cesteros, F. Medina and J. E. Sueiras, *Appl. Catal., A*, 2009, **368**, 163.
- J. A. Melero, G. D. Stucky, R. van Grieken and G. Morales, *J. Mater. Chem.*, 2002, **12**, 1664.

- 32 M. E. Jamróz, M. Jarosz, J. Witowska-Jarosz, E. Bednarek, W. Tecza, M. H. Jamróz, J. C. Dobrowolski and J. Kijenski, *Spectrochim. Acta, Part A*, 2007, **67**, 980.
- 33 J. H. De Boer, in *The Structure and Properties of Porous Materials*, Butterworth, London, 1958.
- 34 J. M. Newsam, M. M. Treacy, W. T. Koetsier and C. B. DeGruyter, *Proc. R. Soc. London, Ser. A*, 1988, **420**, 375.
- 35 W. M. Meiwier, *Z. Kristallogr.*, 1961, **115**, 439.
- 36 M. Müller, G. Harvey and R. Prins, *Microporous Mesoporous Mater.*, 2000, **34**, 135.
- 37 S. Moreno and G. Poncelet, *Microporous Mater.*, 1997, **12**, 197.
- 38 K. H. Chung, *Microporous Mesoporous Mater.*, 2008, **111**, 544.
- 39 D. M. Roberge, H. Hausmann and W. F. Hölderich, *Phys. Chem. Chem. Phys.*, 2002, **4**, 3128.
- 40 E. Cano-Serrano, G. Blanco-Brieva, J. M. Campos-Martin and J. L. G. Fierro, *Langmuir*, 2003, **19**, 7621.
- 41 Y. Kim, Y. Choi, H. K. Kim and J. S. Lee, *J. Power Sources*, 2010, **195**, 4653.
- 42 D. H. Lee, M. Choi, B. W. Yu and R. Ryoo, *Chem. Commun.*, 2009, 74.
- 43 L. E. Marxwell and W. H. J. Stork, in *Introduction to Zeolite Science and Practice, Studies in Surface Science and Catalysis*, ed. H. Van Bekkum, E. M. Flanigen, P. A. Jacobs and J. C. Jansen, Elsevier Science, Amsterdam, 2001, vol. 137.